Electrohydrodynamic Convection in Nematics

L. Kramer, W. Pesch

Universität Bayreuth, D-95447 Bayreuth, Germany

I. INTRODUCTION

Electrohydrodynamic convection (or, briefly, electroconvection, EC) occurs when a voltage above a critical threshold strength is applied across a thin layer of a nematic liquid crystal (nematic) with nonvanishing conductivity [1–7]. At onset one observes typically periodic patterns of convection rolls (see Fig.1). With increasing voltage transitions take place either to rather complex spatio-temporal states, which are heavily influenced by defects or, under appropriate conditions, to more complicated (quasi-)stationary patterns, typically periodic in two directions. Eventually one arrives at turbulent states, which are characterised by strong light scattering (dynamic scattering mode, DMS [8]).

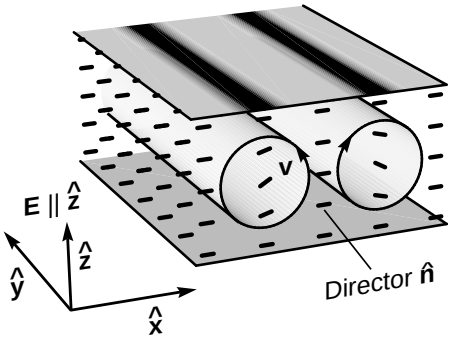

Fig.1a. Cell geometry with section of a roll pattern for EC (planar configuration). **E** = electric field, **v**= velocity.

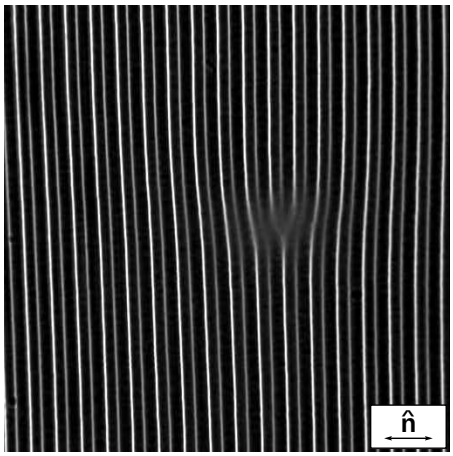

Fig.1b. Normal roll pattern for EC with a dislocation (courtesy I. Rehberg).

After the first systematic experimental characterisation of EC in 1963 by Williams [9] and Kapustin and Larinova [10] the phenomenon has been intensively investigated in the early '70th. In the last 15 years EC in nematics has developed into an important model system for pattern formation in hydrodynamic instabilities [11]. The specific anisotropy of nematics brings out totally new phenomena compared to the canonical example of Rayleigh-Bénard convection in simple fluids [12].

From an experimental point of view EC is, up to some point, a convenient system: simple, multiple control (e.g. amplitude and frequency of voltage, additional magnetic field), convenient time scales, and easy visualisation of the gross features. Limitations result from limited accuracy, reproducibility and optical resolution as well as from the lack of 3D visualisation of the director field inside the layer.

From a theoretical point of view the picture is also two-fold: The full hydrodynamic description (see next section) is mostly well established and transparent, whereas extracting the consequences of its various competing mechanisms is highly demanding. A complete description of the onset behaviour is now feasible (Sec III). On the nonlinear level there is also considerable progress in understanding the secondary instabilities of the roll pattern and more complex states (Sec.IV). The problem has been treated by purely numerical methods, but also by a description in terms of appropriate order parameters. In comparison to full hydrodynamics they satisfy much simpler equations, which can be approached even phenomenologically. The reduced level of order parameter equations allows valuable analytical insight and by numerical simulations, e.g. the description of defects and other spatio-temporal disordered states.

A problem that touches both, experiment and theory, is connected with the large number of material parameters involved in the hydrodynamic description. There are only two room temperature nematics with negative dielectric anisotropy where all the material parameters have been measured: MBBA, see [13], and Merck Phase 5, see [14] (and references therein). Since these nematics are similar in their properties, the investigation of other classes is highly desirable and promising. A recent successful example is the very stable material I52 doped with iodine [15]. Even at onset qualitatively new localised structures ("worms") [16] have been detected, which provide a new challenge for the theory. This applies also to materials where one can shift continuously from the nematic to the smectic phase by decreasing continuously the temperature [17].

II. BASIC EQUATIONS AND INSTABILITY MECHANISMS

The dynamics of nematics is described by a set of macroscopic equations (see e.g. [2,18,19]), which couple the director $\mathbf{n}$, the velocity field $\mathbf{v}$ and the (static or low-frequency) electric and magnetic fields $\mathbf{E}$, $\mathbf{H}$.

The rate equation for the director can be written as (we use $\partial_j = \partial x_j$)

$$\frac{dn_i}{dt} = \Omega_{ki} n_k + \lambda(\delta_{ij} - n_i n_j) A_{jk} n_k + \frac{h_i}{\gamma_1}, \quad \text{where} \qquad \frac{d}{dt} = \partial_t + \mathbf{v}\cdot\nabla, \tag{1}$$

$$\Omega_{ik} = \frac{1}{2}(\partial_i v_k - \partial_k v_i), \quad A_{ik} = \frac{1}{2}(\partial_i v_k + \partial_k v_i), \quad h_i = (\delta_{ij} - n_i n_j)(\partial_k \pi_{kj} - \frac{dF_d}{dn_j}), \quad \pi_{kj} = \frac{\partial F_d}{\partial(\partial_k n_j)}. \tag{2}$$

$\lambda = -\gamma_2/\gamma_1$ is the flow-alignment parameter (≈ 1 for ordinary nematics). The orientational free energy density is given by

$$F_d = K_{11}(\nabla\cdot\mathbf{n})^2 + K_{22}[\mathbf{n}\cdot(\nabla\times\mathbf{n})]^2 + K_{33}[\mathbf{n}\times(\nabla\times\mathbf{n})]^2 - \frac{1}{2}\chi_a(\mathbf{n}\cdot\mathbf{B})^2 - \tag{3}$$

$$- \frac{1}{2}\epsilon_a(\mathbf{n}\cdot\mathbf{E})^2 - \mathbf{P}^{flexo}\cdot\mathbf{E}, \qquad \mathbf{P}^{flexo} = e_1\mathbf{n}(\nabla\cdot\mathbf{n}) + e_3(\mathbf{n}\cdot\nabla)\mathbf{n}. \tag{4}$$

with the orientational elastic modules K_{11}, K_{22}, K_{33} describing the three basic deformations splay, twist and bend of the director field ($K_{ii} \sim 10^{-11}$ kg). χ_a and ϵ_a are the anisotropic parts of the magnetic and electric susceptibilities. A distortion of the director field leads to an electric polarisation P^{flexo} ("flexoeffect") with the flexoelectric coefficients e_1, e_3, which are hard to measure. In Eq.(1) only the last contribution is dissipative (irreversible).

The momentum balance equation (generalised Navier-Stokes equation) and (approximate) incompressibility are given by

$$\rho\frac{dv_i}{dt} = -\partial_i p + \partial_k(\sigma^R_{ik} + \sigma'_{ik} + E_i D_k), \qquad \nabla\cdot\mathbf{v} = 0, \quad \text{where} \tag{5}$$

$$\sigma^R_{ik} = -\pi_{kj}\partial_i n_j + \frac{\alpha_2}{\gamma_1} n_k h_i + \frac{\alpha_3}{\gamma_1} n_i h_k, \quad D_i = \epsilon_{ik}E_k + P_i^{flexo}, \quad \epsilon_{ik} = \epsilon_\perp\delta_{ik} + \epsilon_a n_i n_k. \tag{6}$$

The viscous part of the stress tensor can be written as

$$\sigma'_{ik} = \alpha_4 A_{ik} + (\alpha_6 + \lambda\alpha_3)(n_i n_j A_{jk} + n_k n_j A_{ji}) + (\alpha_1 - \lambda(\alpha_2 + \alpha_3))n_i n_k n_j n_l A_{jl}. \quad (7)$$

Thus one has three independent shear viscosities and the two parameters which characterise the orientational behaviour ($\gamma_1 = \alpha_3 - \alpha_2$, $\gamma_2 = \alpha_3 + \alpha_2$). We note that in the usual Leslie-Ericksen formulation the last two terms in σ^R_{ik} appear together with the viscous terms, which from a systematic point of view may be less appealing. σ^R_{ik} can be symmetrised by adding terms that do not change the body force $\partial_k \sigma_{ik}$ [19–21]. For the occurrence of EC a nonzero conductivity is essential. One may (or even must) add an ionisable dopant to the LC in order to obtain sufficient and/or well-controlled conductivity. Then the following quasi-static Maxwell equations determine the current $\mathbf{J}$ and the charge density ρ_{el}

$$\frac{d\rho_{el}}{dt} = -\nabla \cdot \mathbf{J}, \quad \nabla \cdot \mathbf{D} = \rho_{el}. \quad (8)$$

The condition $\nabla \times \mathbf{E} = 0$ is used to introduce an electric potential. In the "standard model" of EC one assumes Ohm's law

$$J_i = \sigma_{ik} E_k, \quad \sigma_{ik} = \sigma_\perp \sigma'_{ik}, \quad \sigma'_{ik} = (\delta_{ik} + \sigma'_a n_i n_k), \quad (9)$$

to hold, with fixed, anisotropic conductivity. Diffusion currents are usually negligible. From Eqs.(8,9) it can be seen that, as long as $\sigma_a/\sigma_\perp \neq \epsilon_a/\epsilon_\perp$ holds, any spatial variation of the director in the presence of an electric field (i.e. when a current is flowing) leads to the generation of nonzero ρ_{el}. This is an intrinsic property of any anisotropic and inhomogeneous conductor.

Now we can appreciate the main driving mechanism for EC. The important point is that in almost all nematics σ'_a is substantially positive. Choosing materials with negative or only slightly positive dielectric anisotropy ϵ_a (here the materials show great diversity) one easily sees that charges are generated ("focused") at locations where the director bends. The Coulomb force $\rho_{el}\mathbf{E}$ inherent in the term $\partial_k(E_i D_k)$ in Eq.(5) will then drive a velocity field $\mathbf{v}$. Via flow-alignment coupling this enhances the spatial variation of the director and thus generates a positive feedback. Above some threshold V_c this will overcome the stabilising elastic and viscous forces. For typical materials at low frequencies (usually ac driving is used) the threshold voltage is of the order $V_0 = \sqrt{\pi^2 k_{11}/\epsilon_\perp}$. The introduction of the reduced control parameter $R = V^2/V_0^2$ is often useful. When ϵ_a becomes too positive a bend Fréedericksz transition will preempt EC [13].

The SM has three typical (linear) time scales associated with the three dynamical equations shown above: The director relaxation time $\tau_d = \gamma_1 d^2/(K_{11}\pi^2) \sim 1s$, the viscous diffusion time $\tau_v = \rho d^2/\alpha_4 \sim 10^{-5}s$ (d = thickness of the layer $\sim 10 - 100\mu$), and the charge relaxation time $\tau_q = \epsilon_\perp/\sigma_\perp \sim 10^{-2}s$. In the frequency ranges usually covered the effect of viscous relaxation is a very fast process, so the velocity field can be treated adiabatically, which means dropping the left-hand side in Navier-Stokes equation ("inertial terms"). The flexoeffect is for ac driving of minor relevance, but under dc conditions it is certainly important (see below).

There is a very distinct effect which is not captured by the above standard model, namely the travelling rolls arising via a Hopf bifurcation, often observed at threshold, in particular in thin and clean cells [22]. A rather natural generalisation, where the conduction mechanism via two types of mobile ions (generated by a (slow) dissociation-recombination reaction) is included, has been shown to describe all the experimental results. Then the ion densities n^+ and n^- with $\rho_{el} = e(n^+ - n^-)$ become dynamic variables (e = elementary charge). This may be accommodated in the simplest manner by letting the conductivity $\sigma_\perp = e(\mu^+_\perp n^+ + \mu^-_\perp n^-)$ become a dynamic variable by adding the balance equation

$$\partial_t \sigma_\perp + \boldsymbol{\nabla} \cdot (\boldsymbol{v}\, \sigma_\perp + \mu^+_\perp \mu^-_\perp \underline{\underline{\sigma}}' \boldsymbol{E}\rho) = -\tau^{-1}_{\rm rec} \left(\sigma_\perp - \sigma^{\rm eq}_\perp\right). \quad (10)$$

This description has been called the weak electrolyte model (WEM) [23,24].

III. BEHAVIOUR NEAR THRESHOLD

The theoretical task is to solve the equations presented in the previous section with boundary conditions appropriate for the usual slab geometry (see Fig.1a): the director and the electric potentials are fixed at the confining plates and the velocity vanishes there. The large lateral extension allows the use of periodic boundary conditions, and thus a transformation from position to Fourier space ($\mathbf{x} = (x, y) \rightarrow \mathbf{q} = (\mathbf{q}, \mathbf{p})$) in the horizontal directions is advantageous. Also, the time-periodic driving (ac-frequency ω suggests an expansion in a Fourier series in ωt. The remaining transverse direction (z) can be treated by (truncated) expansions in terms of suitable test functions which satisfy the boundary conditions (Galerkin method). In general one then arrives at highly nonlinear algebraic equations for the expansion coefficients. The resulting solutions have to be tested for stability with respect to general fluctuations [25].

This program is simplified considerably when only the onset of the convection instability is to be determined. At onset certain linear perturbations of the basic (primary) state start to grow exponentially ("linear stability analysis"). One has to analyse an eigenvalue problem, where the eigenvalue $\lambda(\mathbf{q}, R) = \sigma(\mathbf{q}, R) \pm i\Omega(\mathbf{q}, R)$ with the largest real part, determines the growth rate σ and the frequency Ω. The condition $\sigma(\mathbf{q}, R) = 0$ defines the neutral surface $R = R_0(\mathbf{q})$. Minimising $R_0(\mathbf{q})$ with respect to $\mathbf{q}$ gives the threshold $R_c = R_0(\mathbf{q}_c)$ with the critical wavevector $\mathbf{q}_c = (q_c, p_c)$ and the critical frequency $\Omega_c = \Omega(\mathbf{q}_c)$, which vanishes for a stationary bifurcation (the more common case in EC) but differs from zero for a Hopf (oscillatory) bifurcation.

The linear stability analysis within the SM for planarly aligned samples ($\mathbf{n} \parallel \hat{\mathbf{x}}$) has a long history starting with Helfrich [26], who considered the case of dc driving. He chose the wave vector $\mathbf{q} = (q, 0)$ parallel to x ("normal rolls", NRs as in Fig.1) and discarded any z dependence ("1D model"). The resulting growth rate has its maximum at $q = 0$. By *setting* $q = 2\pi/d$ a reasonable low-frequency threshold was obtained. The analysis was generalised to ac driving by the Orsay group [27], who thereby established the increase of the threshold with increasing frequency and found a crossover from the low-frequency conduction mode ("conduction regime" in Fig.2a) to a destabilising mode with opposite time-reflection symmetries at higher frequency (the scale is set by τ_q^{-1}) in the "dielectric regime" [Fig.2a]. This dielectric mode can usually be described well within the 1D model, since its wave number is not determined by the width d but rather by the (intrinsic) orientational diffusion length $\sqrt{K_{33}/(|\alpha_2|\omega)}$. In the dielectric range this length is typically small compared to d and then variations in the z direction are indeed negligible. The threshold voltage $\sim \omega^{1/2}$ is in agreement with many experiments, but is at conflict with some others in particular at very high frequency [4,28,29]. Note, that for materials with positive ϵ_a there exists a competing homogeneous ($q = 0$) splay Fréedericksz destabilisation, so here the threshold curve remains finite at high frequencies [13]. Recently there was renewed interest in the interaction between EC and the Fréedericksz transition, which can also be influenced by an additional vertical magnetic field [30].

Inclusion of the variations in the z direction (2D model), thereby allowing for a complete description of the normal-roll threshold, was initiated by Pikin (dc case with some approximations) [31] and Penz and Ford (dc, rigorous) [32]. The 2D theory gives a good account of the threshold behaviour in the NR regime (i.e. the transition line "normal rolls" in Fig.2a).

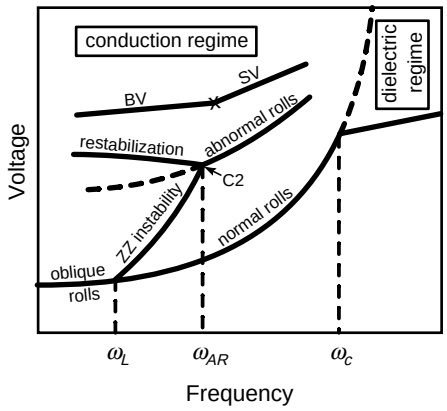

Fig.2a. Schematic stability diagram for planar EC. Convection sets in above the lowest solid curves. For the secondary bifurcations, see text.

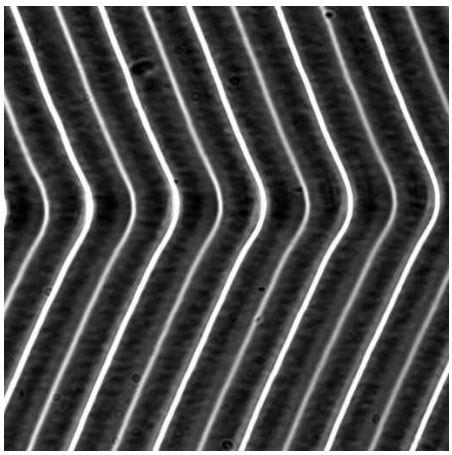

Fig.2b. Zig-zag (ZZ) pattern after increasing the voltage in Fig.1b.

The apparent divergence of the conduction mode threshold at the "cut-off frequency" for negative ϵ_a is a result of the lowest-order time-Fourier expansion. Including higher Fourier modes [33,13] or considering a square-wave voltage, where the problem can be handled essentially analytically [34], it was found that there is in fact restabilisation of the conduction mode at high voltage.

Fifteen years ago, the two most important tasks left for linear theory were understanding the oblique rolls that typically occur at low frequencies and the travelling rolls that appear predominantly in thin and clean cells. The first task proved comparatively simple: The SM, even without inclusion of the flexoeffect, when evaluated properly in 3D, describes the oblique rolls [35,13,36]. The crossover from NRs to oblique rolls occurs at a characteristic codimension-2 point called the Lifshitz point at frequency ω_L. As first shown by Madhusdana et al. [37] in the dc case the flexoeffect provides an additional mechanism for oblique rolls. In the ac case the flexoeffect becomes important only for not too thin and clean cells [36,38]. For a discussion of the dielectric regime, see [39]. Meanwhile there exist computer programs to calculate the threshold curves and the critical wave vector $\mathbf{q}_c$ from the SM to any desired accuracy (with flexoeffect and higher Fourier modes). In addition there exist approximate closed expressions based on one-mode Galerkin expansions which describe satisfactorily the threshold behaviour of the SM over a large parameter range [40].

Understanding the Hopf bifurcation [22] proved more difficult. After all possibilities within the SM were exhausted the WEM was constructed and shown to provide for the Hopf bifurcation. The threshold behaviour in MBBA [41,42], I52 [23] and Phase 5 [14] can be described.

For homeotropic alignment ($\mathbf{n} \parallel \hat{\mathbf{z}}$)one has two very different cases: for negative dielectric anisotropy (not too near to zero) one first has a bend Fréedericksz transition, where the director gains a planar component (planar director $\mathbf{c}$). Increasing the voltage one has eventually a transition to convection, which is, on the linear level, in many ways similar to that in planar cells [43]. The tendency to oblique rolls is enhanced. In Merck Phase 5 one has two Lifshitz points, so that at very low frequency NRs are recovered [44]. For dielectric anisotropy around zero and negative α_3 one has a direct transition to EC with very small wavelength [43].

Very near to a symmetry-breaking bifurcation thermal fluctuations become important. The first clear identification in EC (in fact in any pattern forming instability to our knowledge) was presented in [46] (for recent measurements, see [47]). For their description one has to generalise the hydrodynamic framework, see e.g. [48].

IV. NONLINEAR REGIME

The first task of the nonlinear theory is to describe the saturation of the pattern evolving from the linear modes in the spirit of a (time-dependent) Landau theory. This was achieved by Bodenschatz et al. [13], thereby establishing that the SM leads to a supercritical (continuous) bifurcation. In the oblique-roll regime a superposition of zig and zag rolls leading to rectangular structures is in principle possible, but for small angles of obliqueness this can be excluded by general phenomenological arguments [49].

Next, slow spatial modulations of the ideal periodic pattern with wave vector $\mathbf{q}_c$ can be included in the spirit of a Ginzburg-Landau theory by introducing a complex amplitude A such that the pattern is described by the real part of $A(\mathbf{x})exp(i\mathbf{q}_c\mathbf{x})$. The generic amplitude equation for anisotropic systems in the range of static normal rolls is the real Ginzburg-Landau equation [25]

$$\tau\partial_t A = \left(\epsilon\ - g|A|^2 + r_1\partial_x^2 + r_2\partial_y^2\right) A. \tag{11}$$

Generalisation to the neighbourhood of the Lifshitz point is possible [49]. Deep inside the oblique-roll range one has to use two coupled equations. The coefficients of the amplitude equations were calculated from the SM in [13] (without flexoeffect). The Ginzburg-Landau equations can be used in particular to study the structure and dynamics of dislocations [50] (see Fig.1b) in good agreement with experiments [51]. In this framework the motion of defects provides a a mechanism for the selection of the preferred wavevector $\mathbf{q}_p$. The nonlinear velocity vs. wavevector relation at small mismatch (in fact, there is a logarithmic singularity for $|\mathbf{q}-\mathbf{q}_p| \to 0$) has recently been verified for motion along the rolls [52] and (in a homeotropic systems with a planar magnetic field, see below), perpendicular to the rolls [53].

In the framework of the WEM it was established that the Hopf bifurcation to travelling rolls is supercritical and then one has the complex Ginzburg-Landau equation (actually two or four coupled such equations for the counter-propagating, and possibly oblique, roll systems [54])) to describe the weakly nonlinear behaviour [24]. It turns out that the stationary bifurcation near the crossover to travelling rolls is typically subcritical. The resulting small hysteresis has been measured in various materials [46,55,23]. Particularly interesting scenarios involving extended spatio-temporal chaos at onset [56] and subcritically arising localised structures ("worms") [16] have been found in I52. The former can be understood on the basis of two coupled complex Ginzburg-Landau equations describing zig and zag rolls travelling in the same direction [57]. A phenomenological model has been proposed to describe the worms [58].

To extend the range of validity of the above description finite$-\epsilon$ corrections have to be taken into account (in the following we will often use a reduced voltage $\epsilon = (V^2 - V_c^2)/V_c^2$, with the critical voltage V_c) . Then various higher-order terms appear. In particular the curvature of rolls is known to induce a so called mean flow. In the presence of 2D lateral spatial variations (3D on the hydrodynamic level) the mean flow cannot be fully eliminated due to the singular structure of its spatial dependence. Thus, one is left with an additional (static) equation [59]. Meanwhile there exist efficient computer programs to calculate the coefficients [60,61]. The analysis showed that, at least near to the transition to oblique rolls, normal rolls are destabilised with increasing ϵ by a zigzag (or undulatory) instability (see the "ZZ instability line" in Fig. 2a) as found in experiments [63] (see Fig.2b for a ZZ pattern).

A full numerical Galerkin calculation confirmed this result and extended it to larger ϵ and frequencies [62,60]. Surprisingly, at frequencies above some value $\omega_{AR}(> \omega_L)$ (to the right of $C2$ in Fig. 2a) destabilisation of normal rolls occurs at $\epsilon = \epsilon_{AR}$ via a spatially homogeneous (in the plane of the layer) mode involving a twist of the director. The mode is the analog of that which destabilises the basic state in a twist Fréedericksz transition (magnetic field in the y direction). The instability signalises a (continuous) pitchfork bifurcation from normal to "abnormal rolls" (ARs) where the director attains such a twist deformation, either to the left or to the right. Another interesting effect is the restabilisation of ARs for $\omega < \omega_{AR}$ above

the ϵ_{ARstab} (see the line "restabilization" in Fig. 2a). At larger ϵ the ARs destabilise either via a long-wave skewed-varicose instability (here the modulation wave vector of the destabilising mode is at an oblique angle), or, at smaller frequency, via a short-wave skewed-varicose instability. This is also called a bimodal varicose instability [64,60], because it indicates the transition to a bimodal state composed of the superposition of two roll systems with different orientation.

When one extends this diagram to oblique rolls (wavevector $\mathbf{q} = (q, p)$ with nonzero p, as in Fig. 2b), the AR bifurcation becomes imperfect (smooth), since in oblique rolls the left-right symmetry is already broken. Also, the destabilisation is shifted upward and restabilisation downward, so that the curves meet at some value $P_m(\omega)$ (with vertical slope) [62]. Thus one has an unstable bubble in the $\epsilon - P$ plane which is bounded from below by ϵ_{ZZ}, and from above by ϵ_{ARstab} [40,67]. Thus there is a very interesting codimension-2 (C2) point at $\omega_{AR}, \epsilon_{AR}$.

The reason why ARs had escaped the notice of experimentalists is that in planarly aligned cells and with the ordinary visualisation (at most one polariser in x direction) they cannot be distinguished from NRs. For homeotropic alignment this is different, and there the signature of ARs had indeed been observed before (see below). Indirect evidence comes from the observation of domain walls between the two variants of ARs. They are observable because inside the wall the amplitude of the periodic n_z deformation is larger than in ARs [62]. Meanwhile direct evidence has been obtained from measurements of the ellipticity of the light induced by ARs [65,66]. In these measurements also the ZZ instability, together with the restabilisation line, could be identified. Apparently the rather small width of the system in the x direction, which allowed for 12 roll pairs, stabilised the ZZ structures, which appear above the instability. Interestingly, another line ϵ_{HB} was found, which lies above ϵ_{ARstab} and also goes through the C2 point: whereas the angle of the ZZ structures first increases with ϵ when ϵ_{ZZ} is crossed, it subsequently decreases again, becoming zero at ϵ_{HB}. Then one is left with ARs with domain walls, because the different orientations in the ZZs induce different variants of ARs. The domain walls quickly annihilate and there remains a single AR domain. When one now decreases ϵ, a massive hysteresis occurs: the ARs persist down to ϵ_{ARstab}. Then there is a discontinuous transition to the ZZ branch, which is then followed down.

These features can be understood in terms of a simple, phenomenological description of the AR bifurcation [65,67]. The two active modes involved are the twist mode, characterised by an angle ϕ, and the phase of the roll pattern θ. The equations are

$$\begin{aligned} \partial_t \phi &= (\mu - g\phi^2)\phi + (K_1\partial_x^2 + K_2\partial_y^2)\phi - \gamma\partial_y\theta, \\ \partial_t \theta &= (D_1\partial_x^2 + D_2\partial_y^2)\theta - (\nu + h\phi^2)\partial_y\phi, \end{aligned} \tag{12}$$

The control parameters μ and ν are to be associated with $\epsilon - \epsilon_{AR}$ and $\omega - \omega_{AR}$. The coupling terms are obtained from symmetry considerations. The term proportional to h is included because ν goes through zero. (A similar term in the ϕ equation would allow to include destabilisation of ARs at larger values of μ.) This model contains all the features described above. The slopes of the different lines are easily expressed in terms of the parameters of the model. In particular, for $\nu < 0$, the ZZ instability of NRs at $\mu = (\gamma/D_2)\nu$ preempts the AR instability and ARs exhibit the observed restabilisation. At the HB line there is a heteroclinic connection between ZZ solutions and Wars. Above the LB line domain walls perpendicular to the rolls move spontaneously [67].

This description is well-founded when only modulations along y occur, like in the OZ instability and in OZ solutions. The coefficients can in principle be deduced from hydrodynamics, including (regular) mean flow. In order to describe y and x variations, additional terms that include in particular the singular mean flow have to be included. This changes the re-stabilisation into a skewed-varicose instability and moves it upward [68,61].

Before going to a more general description let us discuss homeotropically aligned systems in materials with

manifestly negative dielectric anisotropy, where one first has a bend Fréedericksz transition through which the director acquires a planar component (planar director **c**). The transition to convection occurring at higher voltage is in many ways similar to that in planar cells, except that the preferred axis (the **c** director) is not externally fixed. Consequently, in a weakly nonlinear description, the Goldstone mode related to rotation of the **c** director has to be included from the beginning on. In generalisation of (11) one then obtains for small angles ϕ, which now denotes the angle between **c** and the x axis [69,70]

$$\begin{aligned} \tau\partial_t A &= \left[\epsilon\ -g|A|^2 + r_1\partial_x^2 + r_2(\partial_y^2 - 2iC_1\phi\partial_y - C_2\phi^2 - i\nu\,\partial_y\phi)\right] A, \\ \partial_t\phi &= G(iq_c\,A^*(\partial_y - iq_c\phi)A + c.c) - T\phi + (K_1\partial_x^2 + K_2\partial_y^2)\phi. \end{aligned} \tag{13}$$

with $C_1 = C_2 = 1$ (we introduce the coefficients for later purpose). Then the first three terms in the bracket proportional to r_2 can be combined to a full square, which expresses (local) invariance with respect to rotation of the rolls together with **c**. If this were an equilibrium system derivable from a potential, then one would need $\nu = 1$. Here, however, ν is an independent coefficient that can (and will, for $\omega < \omega_{AR}$) even become negative. The first term in the $\phi-$equation expresses the "abnormal torque" on the **c** director ($G > 0$!), which arises at second order in the convection amplitude. We have included a (small) linear damping, which appears only in the presence of an additional planar magnetic field (then $T \approx \chi_a H^2$). For $T = 0$ all roll solutions are unstable. In simulations ϕ grows without bounds (for $C_1 = C_2 = 1$!), and then a globally invariant generalisation of these equations must be used, which exhibits dynamic disorder (defect turbulence) [69,70], which is essentially what is found experimentally [71–73].

For $T > 0$ (nonzero planar field) Eqs.(13) describe NRs at band center ($|A| = \sqrt{\epsilon/g},\ \phi = 0$), which are stable against homogeneous ϕ perturbations for $\epsilon < \epsilon_{AR} = T/(2G)$ and against ZZ fluctuations for $\epsilon < \epsilon_{ZZ} = \epsilon_{AR}/(1-\nu)$. Thus, one has a similar situation as in planar cells with the near-Goldstone mode in homeotropic systems corresponding to the twist mode in planar cells. Here, for $C_1 = C_2 = 1$, the ARs $A = \sqrt{\epsilon_{AR}/g},\ \phi = \sqrt{(\epsilon - \epsilon_{AR}}/(r_1 q_c)$ destabilise for $\nu > 0$ at $\epsilon = 3/2\epsilon_{AR}$. There is no restabilisation for $\nu < 0$ because the short-wave instability sets in right at the restabilisation line (also at $\epsilon = 3/2\epsilon_{AR}$). For larger values of ϵ one has dynamic disorder (defect turbulence). In this system ARs are easily identified by birefringence measurements, and the symmetry breaking was indeed first detected in such a system (with $H = 0$) in the disordered state [71]. Meanwhile a quantitative comparison of the pitchfork bifurcation to ARs ($H \neq 0$) with theory has been made [44].

For $\epsilon >> \epsilon_{AR}$ (this can be achieved for any positive value of ϵ by choosing the planar field sufficiently small) one has a spontaneous ordering of defects along periodically arranged lines, which appears to explain the most common types of chevrons observed in the dielectric range of planarly aligned cells [**?**]. The theory is indeed applicable to the dielectric range because here the orienting effects of the boundaries can be considered as small perturbations [39], which is consistent with experiments [74,75]. The prediction that chevrons should occur in homeotropic systems also in the conduction range has been verified [72,73].

Let us now come back to the case of planar alignment. The scenario found there can be described qualitatively by Eqs.(13) with $1 \geq C_2^2 > C_1$. The surface anchoring now leads to $T \approx \chi_a H_F^2$ (H_F=twist Fréedericksz field). The destabilisation of NRs is independent of $C_1,\ C_2$. For negative ν one has a restabilisation curve for ARs which passes through the C2 point with slope $d\epsilon/d\nu = -1/(2(1-C_1))$ and saturates for $\nu \to -\infty$ at $\epsilon_\infty = C_2/(2C_1 + C_2)$. Destabilisation of ARs at large ϵ is also captured. For negative values of ν there is a short-wave instability merging with a long-wave instability curve at some positive ν (for $C_1,\ C_2 \to 1$ this point becomes $\nu = 0,\ \epsilon = 3/2\epsilon_{AR}$). For $\nu \to \infty$ the instability curve tends to ϵ_∞ from above. In the range of stable ARs the equations describe interesting defect scenarios. For $\epsilon >> \epsilon_{AR}$ they describe the dynamic chevrons mentioned before and also a new type of static chevrons [68] (at larger ϵ). The equations can be taken as a quantitative description only when the AR bifurcation occurs sufficiently near to the primary instability. This can be achieved in planar systems by applying an additional (destabilising) magnetic field

in the y direction. Then $T \approx \chi_a(H_F^2 - H^2)$ so that for $H \to H_F$ T, and therefore also ϵ_{AR}, tends to zero for $H \to H_F$. In simulations ϕ remains bounded even for $T = 0$, in contrast to the rotationally invariant case.

When ϵ_{AR} is not sufficiently small, as is the case for planar systems without additional magnetic field, corrections have to be included, which in particular involve mean flow. This has been carried out for the case with modulations only in the y direction [60] (as mentioned before, mean flow can then be eliminated leading to important higher-order terms in the A equation). Otherwise the equations become rather complicated [68,61].

Some of the above studies have been carried over to the oblique-roll regime [69,70,62,60]. The signature of the twist mode (like in ARs) has also been observed in travelling rolls [76].

V. CONCLUDING REMARKS

Although EC in nematics has come a long way since the early days there remains much to do. There are unsolved problems concerning the threshold behaviour of materials near a nematic smectic transition. It appears that in a region where σ_a' has become negative one can get EC in the form of localised structures (worms) [17,77]. In highly doped MBBA [28,78,73] and other materials [29,79] one finds at high frequency a stationary periodic domain structure (period $\sim$ cell thickness), often without detectable convection rolls. The structure appears to persist at least in some cases with increasing temperature up to the nematic-isotropic phase transition. In the "swallow tailed" compounds used in [29] a treatment of the bounding plates by ten-sides led to a considerable increase of the frequency range, where the domains appeared. The periodic behaviour of the in-plane director reminds of chevrons, but the origin is at present not clear (see also [39]).

There are various complex structures which are as yet only partially understood, see e.g. [80,81]. Because of space limitations we have concentrated on the basic phenomena in standard EHC. There exist various other interesting possibilities, which have been mentioned in previous reviews [40,7]. Of particular interest are the use of a periodic modulation of the driving ac-voltage [41,82,76] and superposing noise [83]. It should also be mentioned, that EC in small aspect-ratio systems (very few short rolls) yields interesting bifurcation scenarios [84]. Finally, it would certainly be rewarding to understand better electroconvectively driven turbulence, i.e. the so-called dynamic scattering modes [8].

---

[1] L. M. Blinov, *Electrooptical and Magnetooptical Properties of Liquid Crystals*, John Wiley, (New York 1983).

[2] P. de Gennes and J. Prost, *The Physics of Liquid Crystals*, Clarendon Press, (Oxford 1993).

[3] S. Chandrasekhar, *Liquid Crystals*, University Press, (Cambridge 1992).

[4] S. A. Pikin, *Structural Transformations in Liquid Crystals*, Gordon and Breach Science Publishers, (New York 1991).

[5] L. Kramer and W. Pesch, Annu. Rev. Fluid Mech. **27**, 515 (1995)

[6] For a recent review see A. Buka and L. Kramer, *Pattern formation in liquid crystals* (Springer-Verlag, New-York, 1996).

[7] W. Pesch and U. Behn in "Evolution of Spontaneous Structures in Dissipative Continuous Systems" F. H. Busse and S. C. Müller, eds., Springer, 1998

[8] S. Kai and W. Zimmermann, Prog. Theor. Phys. Suppl. **99**, 458 (1989).

[9] R. Williams, J.Chem.Phys **39**, 384 (1963).

[10] A. Kapustin and L. Larinova, Kristallografya **9**, 297 (1963).

[11] M. C. Cross and P. C. Hohenberg, Rev. Mod. Phys. **65**, 851 (1993).

[12] L. Bodenschatz, W. Pesch and G. Ahlers, Annu. Rev. Fluid Mech. **32**, 709 (2000)

[13] E. Bodenschatz, W. Zimmermann, and L. Kramer, J. Phys.(Paris) **49**, 1875 (1988)

[14] M. Treiber, N. Eber, Á. Buka, and L. Kramer, J. Phys. France II **7**, 649–661 (1997)

[15] M. Dennin, G. Ahlers, and D. Cannell, in P. Cladis and P. Palffy-Muhoray, editors, *Spatio-temporal patterns in nonequilibrium complex systems*, Santa Fe Institute Studies in the Sciences of Complexity **XXI**, Addison-Wesley, New York, (1994); M. Dennin, D. Cannell, and G. Ahlers, Mol. Cryst. Liq. Cryst. **261**, 337 (1995).

[16] M. Dennin, G. Ahlers, and D. S. Cannell, Phys. Rev. Lett. **77**, 2475 (1996); Science **272**, 388 (1997); U. Bisang and G. Ahlers, Phys. Rev. Lett. **80**, 3061 (1998); Phys. Rev. E **60**, 3910 (1999).

[17] H. R. Brand, C. Fradin, P. L. Finn, W. Pesch, and P. E. Cladis, Physics Lett. A **235**, 508 (1997).

[18] M. J. Stephen and J. P. Straley, Rev. Mod. Phys. **46**, 617 (1974).

[19] See the contribution of H. Pleiner and H. Brandt in [6].

[20] L.D. Landau and E.M. Lifshitz, Lehrbuch der Theoretischen Physik,Vol. 7, Akadamie Verlag, (Berlin, 1989)

[21] D. Forster, T. Lubensky, P. C. Martin, J. Smith and P.J. Pershan, Phys.Rev.Lett. **26**, 1016 (1971); P. C. Martin, O. Parodi and P.J. Pershan **A6**, 2401 (1972).

[22] S. Kai and K. Hirakawa, Prog. Theor. Phys.Suppl. **14**, 212 (1978); A. Joets and R. Ribotta, Phys. Rev. Lett. **60**, 2164(1988); I. Rehberg, S. Rasenat, and V. Steinberg, Phys. Rev. Lett. **62**, 756 (1989).

[23] M. Dennin, M. Treiber, L. Kramer, G. Ahlers, and D. Cannell, Phys. Rev. Lett. **76**, 319 (1996).

[24] M. Treiber and L. Kramer, Phys. Rev. E **58**, 1973 (1998).

[25] See the contribution of W. Pesch and L. Kramer in [6].

[26] W. Helfrich, J. Chem. Phys. **51**, 4092 (1969).

[27] E. Dubois-Violette, P. G. de Gennes, and O. J. Parodi, J. Phys.(Paris) **32**, 305 (1971). E. Dubois-Violette, G. Durand, E. Guyon, P. Manneville amd P. Pieranski, in *Solid State Physics, Supplement 14* (1978)

[28] A.N. Trufanov, L.M. Blinov, and M.I. Barnik, in *Advances in Liquid Crystal Research and Applications*, L. Bata, ed. (Pergamon Press, Oxford-Budapest, 1980), p.549.

[29] W. Weissflog, G. Pelzl H. Kresse, and D. Demus, Crystal Research and Technology **23**, 1259 (1988).

[30] A. Hertrich, W. Pesch, and J. T. Gleeson, Europhys. Lett. **44**, 417 (1996).

[31] S.A. Pikin, Zh. Eksp. Teor. PFiz. **60**, 1185 (1971) [Sov. Phys.-JETP **33**, 641 (1971)].

[32] P.A. Penz and G.W. Ford, Phys. Rev. **A 6**, 414 (1972).

[33] P. Sengupta and A. Saupe, Phys. Rev. **A 9**, 2698 (1974).

[34] E. Dubois-Violette, J. Phys.(Paris) **33**, 95 (1972); R.A. Rigopoulos and H.M. Zenginoglou, Mol. Cryst. Liq. Cryst. **35**, 307 (1976).

[35] W. Zimmermann and L. Kramer, Phys. Rev. Lett. **55**, 402 (1985).

[36] L. Kramer, E. Bodenschatz, W. Pesch, W. Thom, and W. Zimmermann, Liquid Crystals **5**(2), 699 (1989).

[37] N. V. Madhusudana, V. A. Raghunathan, and K. R. Sumathy, Pramāna, J. Phys. **28**, L311 (1987).

[38] The importance od the flexoeffect for the appearance of oblique rolls is overrated in [3], p.210 and in L. M. Blinov and V. G. Chigrinov, *Electrooptical and Magnetooptical Properties of Liquid Crystal materials*, Springer, (New York 1996), p.263.

[39] A.G. Rossberg, *Three-dimensional pattern formation, multiple homogeneous soft modes, and nonlinear dielectric electroconvection*, preprint, http://arXiv.org/abs/nlin/?0001065 (2000)

[40] See the contribution of L. Kramer and W. Pesch in [6].

[41] I. Rehberg, S. Rasenat, J. Fineberg, M. del la Torre Juarez, and V. Steinberg, Phys. Rev. Lett. **61**, 2449 (1988).

[42] M. Treiber, PhD thesis, Universität Bayreuth, (1996).

[43] A. Hertrich, W. Decker, W. Pesch, and L. Kramer, J. Phys. France **II 2**, 1915 (1992); L. Kramer, A. Hertrich, and W. Pesch, in *Pattern formation in complex dissipitative systems*, S. Kai, ed. (World Scientific, Singapore, 1992) p. 238.

[44] A.R. Rossberg, N. Eber, A. Buka and L. Kramer , Phys. Rev. E, **61** , R25 (2000)

[45] L. Kramer, A. Hertrich, and W. Pesch, in *Pattern formation in complex dissipitative systems*, S. Kai, ed. (World Scientific, Singapore, 1992) p. 238.

[46] I. Rehberg, S. Rasenat, M. de la Torre Juarez, W. Schöpf, F. Hörner, G. Ahlers, and H. Brand, Phys.Rev.Lett **67**, 596 (1991).

[47] M. A. Scherer, G. Ahlers, F. Hörner and I. Rehberg, *Deviations from linear theory for fluctuatuins below the supercritical primary bifurcation to electroconvection*, preprint (2000).

[48] See the contribution of M. Treiber in [6].

[49] W. Pesch and L.Kramer, Z.Phys. B **63**, 121 (1986);

[50] E. Bodenschatz, W. Pesch and L. Kramer, Physica D **32**, 135 (1988) E. Bodenschatz, A. Weber, and L. Kramer, J. Stat. Phys. **64**, 1007 (1991).

[51] L. Kramer, E. Bodenschatz and W. Pesch, Phys. Rev. Lett. **64**, 2588 (1990).

[52] V. Steinberg, private communication.

[53] P. Toth, N.Eber, L.Kramer, and A. Buka, to be published.

[54] M. Silber, H. Riecke und L. Kramer, Physica D **61**, 260 (1992)

[55] I. Rehberg, F. Hörner and H. Hartung, J. Sta. Phys. **64**, 1017 (1991)

[56] M. Dennin, D. S. Cannell and G. Ahlers,, Phys. Rev. E **57**, 638 (1997)

[57] H. Riecke and L. Kramer, Physica D **137**, 124 (2000)

.

[58] H.Riecke and G.D. Granzow , Phys. Rev. Lett **81**, 333 (1998)

[59] M. Kaiser and W. Pesch, Phys. Rev. E **48**, 4510 (1993).

[60] E. Plaut and W. Pesch, Phys.Rev.E, **59**, 1247 (1999)

[61] B. Dressel and W. Pesch, unpublished.

[62] E. Plaut, W. Decker, A. Rossberg, L. Kramer, W. Pesch, A. Belaidi, and R. Ribotta, Phys. Rev. Lett. **79**, 2376, (1997).

[63] A. Joets and R. Ribotta, J. Phys.(Paris) **47**, 595 (1986); E. Braun, S. Rasenat, and V. Steinberg, Europhys. Lett. **15**, 597 (1991). S. Nasuno and S. Kai, Europhys. Lett. **14**, 779 (1991); S. Nasuno, O. Sasaki, S. Kai, and W. Zimmermann, Phys. Rev. A. **46**, 4954 (1992).

[64] E. Plaut and R. Ribotta , Europhys. Lett. **38**, 441 (1997).

[65] H. Zhao, L. Kramer, I. Rehberg, and A. Rudroff. Phys. Rev. Lett. **81** , 4144 (1998).a

[66] S. Rudroff, V. Frette and I. Rehberg, Phys. Rev. E **59**, 1814 (1999)

[67] H. Zhao and L. Kramer, Phys. Rev. E, in press.

[68] H. Zhao , PhD thesis, Bayreuth 2000.

[69] A. G. Rossberg, A. Hertrich, L. Kramer, and W. Pesch, Phys. Rev. Lett. **76**, 4729–4732 (1996).

[70] A.G. Rossberg, PhD thesis, Bayreuth 1998 ; A.G. Rossberg and L. Kramer, Physica Scripta, **T67** 121 (1996)

[71] H.Richter, A.Buka, and I.Rehberg, in P. Cladis and P. Palffy-Muhoray, editors, *Spatio-temporal patterns in nonequilibrium complex systems*, Santa Fe Institute Studies in the Sciences of Complexity **XXI**, Addison-Wesley, New York, (1994).

[72] P. Toth, A. Buka, J. Peinke and L. Kramer, Phys. Rev. E **58** (1998)

[73] J. H. Hu and Y. Hidaka, A. G. Rossberg and S. Kai, Phys. Rev. E **61**, 2769 (2000)

[74] A. G. Rossberg and L. Kramer, Physca D **115**, 19 (1998)

[75] M. Scheuring, L. Kramer und J. Peinke, Phys. Rev. E**58**, 2018 (1998).

[76] H. Amm, R. Stannarius, and A. G. Roßberg, Physica D**126**, 171 (1999).

[77] M. Dennin, *Direct observation of twist mode in electroconvection in I52* , preprint, http://arXiv.org/abs/cond-mat/0003515 (2000).

[78] C.F. Fradin, P.L. Finn, P. Cladis and H.R. Brand, Phys. Rev. Lett **81**, 2902 (1998)

[79] L. Nasta, L. Lupu, and M. Giurgea, Mol. Cryst. Liq. Cryst. **71**, 65 (1981).

[80] N. Eber, T. Tóth Katona, A. Buka, private communication.

[81] S. Nasuno, O. Sasaki, S. Kai, and W. Zimmermann, Phys. Rev. A **46**, 4954 (1992).

[82] A. Belaidi and R. Ribotta, *Restabilisation of topological disorder into an ordered lattice of defects*, preprint 1997.

[83] A. Belaidi, PhD thesis, University of Orsay (Paris XII), 1998

[84] Th. John, R. Stannarius, U. Behn, Phys. Rev. Lett. **83**, 749-752 (1999).

[85] T. Peacock, D. J. Binks and T.Mullin, Phys.Rev.Lett. **82**,1446 (1999)